

Generation of polarization entangled photon pairs by a single crystal interferometric source pumped by femtosecond laser pulses

M. Barbieri, C. Cinelli, F. De Martini, P. Mataloni
 Dipartimento di Fisica, Università di Roma "La Sapienza"
 and Consorzio Interuniversitario
 per le Scienze Fisiche della Materia,
 Roma, 00185 ITALY
 e-mail: paolo.mataloni@uniroma1.it

Abstract

Photon pairs, highly entangled in polarization have been generated under femtosecond laser pulse excitation by a type I crystal source, operating in a single arm interferometric scheme. The relevant effects of temporal walk-off existing in these conditions between the ordinary and extraordinary photons were experimentally investigated. By introducing a suitable temporal compensation between the two orthogonal polarization components highly entangled pulsed states were obtained.

1 Introduction

Quantum states of polarization entangled photons, generated by the Spontaneous Down Conversion (SPDC) process, are widely used for the realization of important tasks of quantum information and are proposed for several schemes of quantum cryptography [1, 2, 3]. Pairs of correlated SPDC photons at wavelenght (wl) λ_A and λ_B and wavevector \mathbf{k}_A and \mathbf{k}_B are generated by a nonlinear (NL) optical crystal shined by a pump leaser beam at wl λ_p and wv \mathbf{k}_p . In presence of polarization, π -entanglement and degenerate

parametric emission ($\lambda_A = \lambda_B = \lambda = \lambda_p/2$) the bipartite 2×2 Hilbert space is spanned by the Bell state basis:

$$|\Psi^\pm\rangle = \frac{1}{\sqrt{2}}(|H_A V_B\rangle \pm |V_A H_B\rangle), \quad (1)$$

$$|\Phi^\pm\rangle = \frac{1}{\sqrt{2}}(|H_A H_B\rangle \pm |V_A V_B\rangle), \quad (2)$$

expressed in the horizontal (H) and vertical (V) polarization basis.

Generally, polarization, π -entangled photon states are generated by a type II noncollinear "phase matched" nonlinear (NL) crystal in which a pair of mutually orthogonally polarized photons is generated over two particular correlated \mathbf{k} modes [4]. The overall quantum state emitted over these two modes is generally expressed by either Bell state $|\Psi^\pm\rangle$, depending on a preset NL crystal orientation. Other sources of π -entangled pairs are based on SPDC radiation generated by coherently pumping two thin type I crystals, orthogonally oriented and placed in mutual contact [5] and by the interferometric parametric source, in which a single type I crystal is excited in two opposite directions (\mathbf{k}_p , $-\mathbf{k}_p$) by a back-reflected pump beam [6]. In both cases the spatial indistinguishability of the two parametric emission cones of the crystals, which are associated to the orthogonal polarizations, H and V , are responsible of the polarization entanglement corresponding to the Bell states $|\Phi^\pm\rangle$. Several examples of two photon state manipulation, allowing the generation of either pure or mixed states, with variable degree of entanglement and mixedness, have been realized [7, 8] by these sources. More recently, their flexibility has been demonstrated in the generation of hyper-entangled photon pairs [9, 10].

A great deal of effort has been devoted towards development of sources of entangled photons operating under *fsec* laser pulse pumping. While this is generally done with type II phase matching [11], only few examples of pulsed entangled state generation have been given for a double crystal system operating in the *fsec* regime [12]. It is well known that in this case temporal walk-off may determine a strong degradation of π -entanglement because of the distinguishability introduced on the photon path-ways by the effects of dispersion and birefringence in the NL crystal [12, 13]. In the present paper we report on the efficient generation of polarization entangled pairs, obtained when the interferometric single crystal scheme [6] operates in this temporal regime. The effects of relevant walk-off affecting the entangled state generation in this particular case have been considered. Moreover, we

have performed a detailed investigation of the properties of entanglement and nonlocality of the parametric source and compared the experimental results with the theoretical predictions.

2 The single crystal interferometric source

2.1 Description

Let's briefly describe the parametric source shown in Figure 1. It is based on a *single arm* interferometer whose active element is given by a single type-I, $l = 0.5mm$ thick, β -barium-borate (BBO) crystal, cut at the phase matching angle $\vartheta = 29.3^\circ$. It is excited in two opposite directions, \mathbf{k}_p and $-\mathbf{k}_p$, by a single transverse mode, vertically (V) polarized, 2^{nd} harmonic beam of a Ti-Sapphire (Coherent, MIRA 900) f sec laser ($\lambda_p = 397.5nm$). The pump beam is slightly focused by a $f = 150\text{ cm}$ lens on the BBO. H polarized degenerate photon pairs are generated at $\lambda = 795\text{ nm}$ over an emission cone with full aperture $\simeq 6^\circ$. The interferometric scheme performs the simultaneous reflection by a common spherical mirror M of either the pump beam or the parametric radiation. It includes also a λ quarter wave plate (λ -qwp) which plays a fundamental role in the generation of the entangled state by performing the $H \rightarrow V$ transformation for the SPDC radiation. This scheme is the same of that previously described in the case of cw pumping operation [6]. After transmission through a $f = 15cm$ lens (L) the photons belonging to the emission cone are transmitted through a circular mask which identifies the so-called *entanglement-ring* ($e - ring$). More than $15 \cdot 10^3$ photon pairs corresponding to the π -entangled state $|\Phi\rangle = \frac{1}{\sqrt{2}}(|H_A H_B\rangle + e^{i\phi} |V_A V_B\rangle)$ are detected for a pump power of $150mW$, within the spectral bandwidth $\Delta\lambda = 3nm$ of the interference filters (IF), which corresponds to a coherence-time of the emitted photons: $\tau_{coh} \approx 447f\text{ sec}$. It is worth noting that a very high phase stability of the state is guaranteed by the particular configuration of single arm interferometer adopted for the source. Indeed, the triplet ($\phi = 0$) to singlet ($\phi = \pi$) state transition is performed by a macroscopic displacement ($\simeq 70\text{ }\mu m$) of mirror M with respect the BBO crystal.

A significant test of the spatial and temporal superposition of the two cones, in absence of polarization entanglement (i.e. with the λ -qwp oriented at 0° with respect its optical axis), is given by the measurement of the interference visibility performed by changing the phase ϕ and detecting an

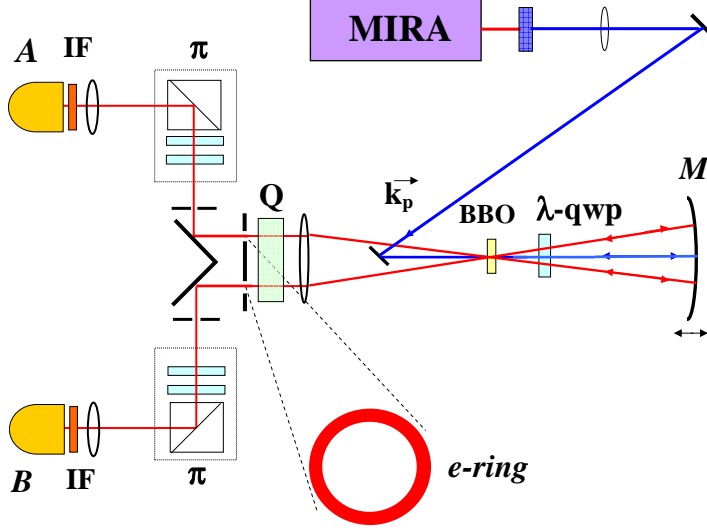


Figure 1: Layout of the source of polarization entangled photon states operating in pulsed regime.

increasing fraction of the e -ring. This condition corresponds to the absence of any temporal or spatial walk-off between the photon pairs which can be generated with equal probability either in the first or in the second passage through the crystal. The single and the coincidence rates vary in this case proportionally to $\cos^2(\frac{\theta}{2})$. We could measure $V \geq 0.9$ over the entire e -ring, while a maximum of $V = 0.93$ was obtained for an arc length of $\simeq 2mm$.

2.2 Temporal and spatial walk-off

The two birefringent (b.r.) elements, represented by the BBO crystal and the λ -qwp, may determine a relevant walk-off between the H and V polarization components when polarization entanglement is performed (i.e. with λ -qwp oriented at 45°). In particular, when passing through a b.r. medium of length x , the temporal walk-off occurring between the ordinary and extraordinary wavepackets, with group velocities v_o and v_e , is

$$\tau = x \left(\frac{1}{v_o} - \frac{1}{v_e} \right)$$

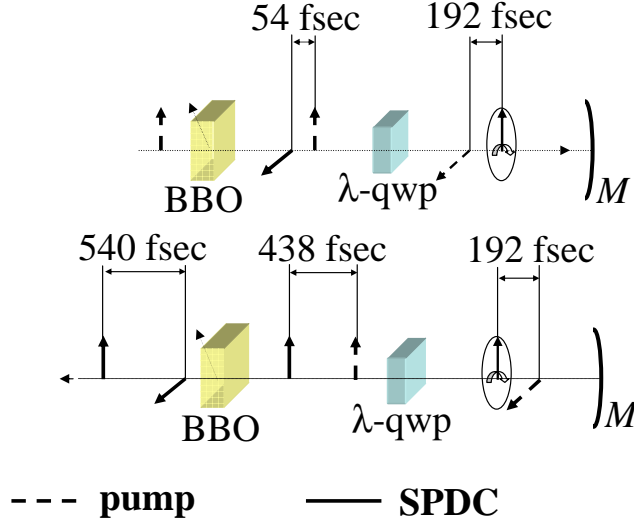


Figure 2: Schematic picture of the temporal delays occurring between the pump and the H and V polarized photons in each section of the parametric source.

We need to consider this effect for each b.r. element present inside the parametric source (in the present case the BBO and the λ -qwp) and compare the resultant value of τ with the coherence-time τ_{coh} .

Spatial walk-off arises from the different output angles at which the two waves go out of each b.r. element. This corresponds to a mutual spatial displacement δ of the two beams, given by

$$\delta = x \tan \alpha \sim x\alpha,$$

where α represents the mutual angle between the two waves. Spatial walk-off becomes particularly severe when δ is of the order of the beam diameter.

Let's evaluate first the temporal walk-off effect. Here we assume that any H polarized photon pair generation event occurs in the center $l/2$ of BBO. Moreover, either the pump pulse or the photon pair generated in the first passage passes two times with their own polarizations through the NL crystal and the zero-order λ -qwp. It is made by putting together two horthogonally oriented quartz crystals, with thickness l' and $l' + \lambda/4$, where $l' = 1.8mm$

[14]. The total temporal walk-off effect can be evaluated by looking at the scheme of Figure 2 which shows how the temporal delay occurring between the pump and the parametric photons varies in each portion of the whole path BBO- M -BBO. Note that, because of the transmission through λ -qwp, SPDC radiation and pump beam are respectively circularly and vertically polarized when travel through the section between M and λ -qwp. In order to evaluate the total temporal walk-off, the following refractive indexes have to be considered [15]:

Refractive index	BBO	Quartz
$n_o(\lambda_p)$	1.69355	1.5585
$n_e(\lambda_p)$	1.59574	1.5681
$n_o(\lambda)$	1.6607	1.5384
$n_e(\lambda)$	1.57013	1.54725

(3)

Note the different sign of birefringence occurring in BBO and quartz..After a round trip, i.e. at the exit of BBO, H -polarized photons are delayed by $\tau = 540f$ sec with respect V -polarized photons. This value determines a strong degradation of entanglement.

Concerning spatial walk-off, it is worth noting that, differently from the type II crystal or the double crystal cases, because of the particular geometry of our source, in the present condition the $|H_A H_B\rangle$ and $|V_A V_B\rangle$ components travel in two parallel directions with a negligible spatial displacement δ when go outside the BBO crystal for the second time.

The above considerations lead us to consider the relevant role of temporal walk-off and discard spatial walk-off in the generation of polarization entanglement. If temporal walk-off is not perfectly compensated the produced state can be expressed by the density matrix:

$$\rho = \frac{1-v}{2} (|H_A H_B\rangle \langle H_A H_B| + |V_A V_B\rangle \langle V_A V_B|) + v |\Phi\rangle \langle \Phi| \quad (4)$$

with $0 \leq v \leq 1$ representing the weight of the entangled state contribution. Temporal walk-off can be compensated by introducing an equal amount of temporal delay of $|V_A V_B\rangle$ with respect the $|H_A H_B\rangle$ component, restoring in this way the temporal indistinguishability. In the next Section we'll examine in detail some experimental results concerning this point.

3 Purification by temporal walk-off compensation

Temporal walk-off can be compensated by a suitable quartz plate with the optical axis oriented in the H direction in order to recover temporal indistinguishability of the $|H_A H_B\rangle$ and $|V_A V_B\rangle$ components. Basing on the values of the ordinary and extraordinary refractive indexes of (3), 18mm of quartz are necessary on this purpose. The plate Q , shown in Figure 1, intercepting the entire $e - ring$, was aligned at the output of the source with the optic axis oriented along the H direction.

We tested the polarization entanglement of the state $|\Phi^+\rangle$ by using the two polarization analyzers (π) shown in Figure 1 before the single photon detector modules (A and B). The experimental data given in Figure 3 show the π -correlation obtained by rotating the first analyzer having kept fixed the axis of the other at 45° . The interference pattern shows the high degree of polarization entanglement of the source. The measured visibility of the coincidence rate, $V \simeq 90\%$, gives a strong indication of the entangled nature of the state over an arc length of 2mm, while the single count rates don't show any periodic fringe behaviour, as expected. A polarization interference visibility $\geq 85\%$ was measured over the entire $e - ring$.

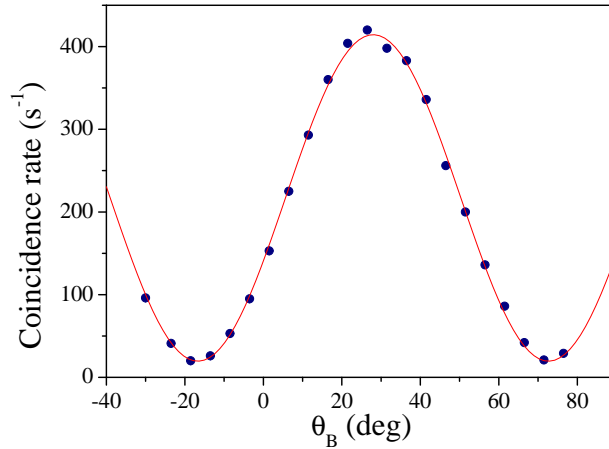


Figure 3: Interference pattern of π -entanglement for the state $|\Phi^+\rangle$, corresponding to a selected arc length of the $e - ring = 2mm$.

A further test of π -entanglement, after compensation of temporal walk-off, is given by the tomographic reconstruction of the state $|\Phi^-\rangle$ shown in Figure 4.

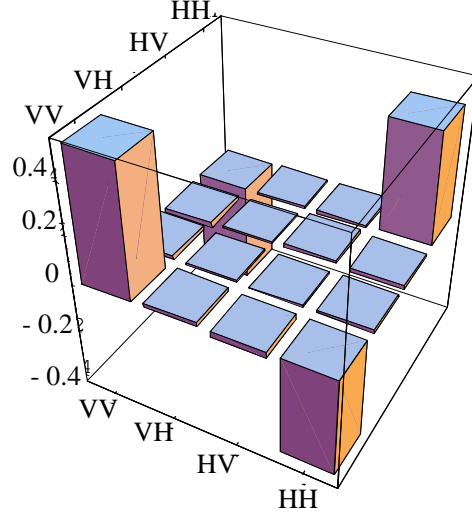


Figure 4: Tomographic reconstruction (real parts) of the state $|\Phi^-\rangle$. The imaginary components are negligible. Tangle $T = 0.974 \pm 0.091$, linear entropy $S_L = 0.031 \pm 0.059$, fidelity $F = 0.949 \pm 0.012$.

Finally, we performed a detailed investigation of the state ρ of Eq. (4) by measuring the entanglement for different quartz plate thicknesses. The experimental results referring to the entanglement visibility V are summarized in Figure 5a and compared with the theoretical predictions. These are obtained by following the theoretical model of Ref. [12] and calculating the convolution of the two photon state amplitude with the gaussian shape of the IF transmission function. As expected, the maximum visibility is obtained for a quartz thickness of $18mm$.

The entanglement witness operator is a method which allows to detect entanglement with few local measurements [16]. For the state ρ , in the case

of the state $|\Phi^+\rangle$, it is given by the expression

$$W = (|\Psi^-\rangle\langle\Psi^-|)^{PT} = \frac{1}{2} \begin{pmatrix} 0 & 0 & 0 & -1 \\ 0 & 1 & 0 & 0 \\ 0 & 0 & 1 & 0 \\ -1 & 0 & 0 & 0 \end{pmatrix}$$

where $|\Psi^-\rangle$ is the eigenvector corresponding to the minimum eigenvalue of the partial transposition (PT) of ρ .

It is obtained

$$\text{Tr}(W\rho) = -\frac{v}{2}$$

which is always negative for any value of $v \neq 0$. The experimental results shown in Figure 5b confirm the theoretical predictions, giving a minimum value $W = -0.3808 \pm 0.0043$ for a quartz thickness of $18mm$.

The last experiment, performed by varying the quartz thickness, consisted of the measurement of the Bell-inequality parameter

$$S = |P(\theta_A, \theta_B) - P(\theta_A, \theta'_B) + P(\theta'_A, \theta_B) + P(\theta'_A, \theta'_B)|, \quad (5)$$

where

$$P(\theta_A, \theta_B) = \frac{[C(\theta_A, \theta_B) + C(\theta_A^\perp, \theta_B^\perp) - C(\theta_A, \theta_B^\perp) - C(\theta_A^\perp, \theta_B)]}{[C(\theta_A, \theta_B) + C(\theta_A^\perp, \theta_B^\perp) + C(\theta_A, \theta_B^\perp) + C(\theta_A^\perp, \theta_B)]}. \quad (6)$$

and $C(\theta_A, \theta_B)$ is the coincidence rate measured by the two detectors and $\theta_A = 0$, $\theta_A^\perp = \pi/2$, $\theta_B = \pi/4$, $\theta_B^\perp = (3/4)\pi$. Figure 5c shows the experimental results. The maximum value $S = 2.465 \pm .012$, corresponding to a violation as large as 38 standard deviations with respect to the local realistic bound $S = 2$, confirms once again the expected maximum for a quartz thickness of $18mm$. It is worth noting that the violation of Bell's inequality is a stronger condition than entanglement. Examples of non separable states which admit a local realistic model can be given [17].

4 Conclusions and acknowledgments

The structural characteristics of a single crystal parametric source of π -entangled photon pairs, based on a single arm interferometer and operating under femtosecond laser pulse excitation, has been described. We have discussed the

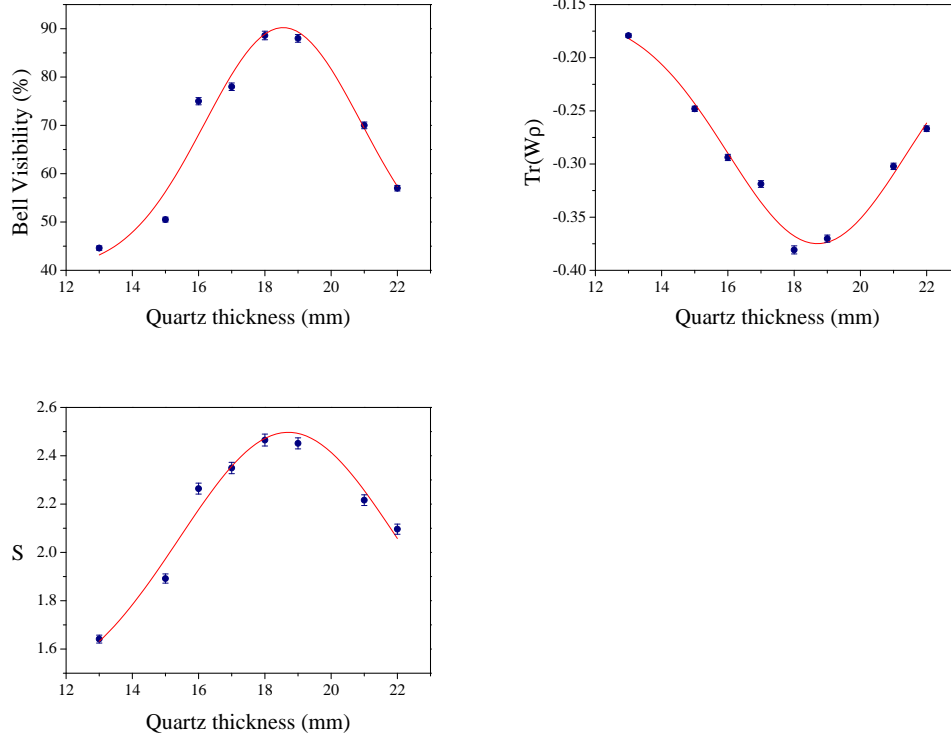


Figure 5: a) Entanglement visibility of the state $|\Phi^+\rangle$ measured for different values of quartz thickness. b) Experimental results of entanglement witness for the state $|\Phi^+\rangle$, measured for different values of quartz thickness. c) Plot of the Bell parameter $|S|$ as a function of quartz thickness.

effects of temporal walk-off existing between the horthogonal polarization components that, in these conditions, strongly affect the purity of the entangled state. Polarization entanglement has been investigated in a detailed way by measuring the state visibility, the entanglement witness operator and the Bell nonlocal parameter $|S|$ as a function of quartz thickness. Highly pure entangled states has been obtained by a suitable compensation of temporal walk-off.

This work was supported by the the FIRB 2001 and PRIN 05 of MIUR (Italy).

References

- [1] A.Ekert, R. Jozsa, R., *Rev. Mod. Phys.* 68, 733 (1996).
- [2] D. Boschi *et al.*, 1998, *Phys. Rev. Lett.* 80, 1121; D. Bouwmeester *et al.*, 1997, *Nature (London)* 390, 575.
- [3] A.Ekert, 1992, *Nature (London)* 358, 14; N. Gisin, G. Ribordy, W. Tittel, and H. Zbinden, 2002, *Rev. Mod. Phys.* 74, 145; A. Ekert, 1991, *Phys. Rev. Lett.* 67, 661.
- [4] P. G. Kwiat, K. Mattle, H. Weinfurter, A. Zeilinger, A. V. Sergienko and Y. Shih 1995, *Phys. Rev. Lett.* 75, 4337.
- [5] P. G. Kwiat, E. Waks, A. G. White, I. Appelbaum and P. H. Eberhard, 1999, *Phys. Rev. A*, 60, R773.
- [6] G. Giorgi, G. Di Nepi, P. Mataloni and F. De Martini, 2003, *Laser Physics*, 13, 350; C. Cinelli, G. Di Nepi, F. De Martini, M. Barbieri and P. Mataloni, 2004, *Phys. Rev. A*, 70, 022321.
- [7] M. Barbieri, F. De Martini, G. Di Nepi, P. Mataloni, 2004, *Phys. Rev. Lett.* 92, 177901.
- [8] N.A. Peters, J.B. Altepeter, D.Branning, E.R. Jeffrey, Tzu-Chieh Wei, and P.G. Kwiat, 2004, *Phys. Rev. Lett.* 92, 133601.
- [9] C. Cinelli, M. Barbieri, R. Perris, P. Mataloni, F. De Martini, 2005, *Phys. Rev. Lett.* 95, 240405.
- [10] J. T. Barreiro, N. K. Langford, N. A. Peters, P. G. Kwiat, 2005, *Phys. Rev. Lett.* 95, 260501.
- [11] D. Bouwmeester, J.-W. Pan, M. Daniell, H. Weinfurter, A. Zeilinger, 1999, *Phys. Rev. Lett.* 82, 1345.
- [12] Y. Nambu, K. Usami, Y. Tsuda, K. Matsumoto and K. Nakamura, 2002, *Phys. Rev. A*, 66, 033816; polarization entanglement has been demonstrated also with two-spatially separated type I crystals pumped by f sec laser pulses, but after amplitude post-selection, by: Y.-H Kim, S.P. Kulik, Y. Shih, 2000, *Phys. Rev. A*, 62, 011802.

- [13] G. Di Giuseppe, L. Haiberger, F. De Martini, A.V. Sergienko, 1997, *Phys. Rev. A*, 56, R21.
- [14] The λ -qwp thickness has been evaluated by measuring the temporal delay induced on the f sec laser pulse ($\lambda = 795nm$) by inserting it in one arm of a Michelson interferometer.
- [15] V.G. Dmitriev, G.G. Gurzadyan, and D. N. Nikogosyan, *Handbook of Nonlinear Optical Crystals* (Springer Series in Optical Sciences, Springer-Verlag, New York, 1999).
- [16] M.Barbieri, F.De Martini, G.Di Nepi, P.Mataloni, G.M.D'Ariano and C.Macchiavello, 2003, *Phys.Rev.Lett.*, 91, 227901
- [17] R. F. Werner, 1989, *Phys. Rev. A* 40, 4277.